Journal of Power Sources 192 (2009) 367–371

Contents lists available at ScienceDirect

Journal of Power Sources

journal homepage: www.elsevier.com/locate/jpowsour

Short communication

Unbiased characterization of three-phase microstructure of porous lanthanum doped strontium manganite/yttria-stabilized zirconia composite cathodes for solid oxide fuel cells using atomic force microscopy and stereology

S. Zhang, M. Lynch, A.M. Gokhale*, M. Liu

School of Materials Science and Engineering, Georgia Institute of Technology, 771 Ferst Drive, Atlanta, GA 30332-0245, United States

ARTICLE INFO

Article history:
Received 4 March 2009
Received in revised form 20 March 2009
Accepted 23 March 2009
Available online 31 March 2009

Keywords:
Porous composite cathode
Microstructure
Triple phase boundaries
Atomic force microscope

ABSTRACT

Microstructural characteristics of porous LSM/YSZ composite cathodes greatly influence the performance of solid oxide fuel cells. The triple phase boundaries, for example, account for a significant portion of the electrochemically active sites in these porous composite cathodes. Nonetheless, experimental characterization of the relevant microstructural attributes has been problematic due to lack of suitable microscopy techniques for simultaneous observations of all three phases (i.e., LSM, YSZ, and porosity) needed for identification and unbiased characterization of the triple phase boundaries. In this contribution it is shown that a combination of chemical etching and atomic force microscopy clearly reveals all three phases and the triple phase junctions in the microstructural sections. Further, stereological techniques based on the geometric probabilities of stochastic geometry enable unbiased statistical estimation of total triple phase boundary length per unit volume and other microstructural attributes from simple counting measurements performed on representative microstructural sections.

1. Introduction and background

Lanthanum doped strontium manganite (LSM) is the most widely used cathode for solid oxide fuel cells (SOFC) based on yttria-stabilized zirconia (YSZ) electrolyte because of its excellent chemical and thermal compatibility with YSZ. Nonetheless, the catalytic activity of LSM is severely limited by its poor ionic conductivity, especially at low operating temperatures. Consequently, in the LSM/YSZ cathodes, the electrochemically active sites for oxygen reduction reactions are mostly at the triple phase boundaries (TPB), which are the lineal regions common to the LSM, YSZ, and air (porosity). As a result, porous composites containing LSM and an ionic conductor such as YSZ have been used to increase the active reaction sites for oxygen reduction reactions via an increase in the total length of the TPB per unit volume in the microstructure [1–4]. It follows that the electrochemical performance of such porous composite cathodes is microstructure sensitive.

The LSM/YSZ composite cathodes are typically fabricated using powder processing techniques involving printing or spraying and sintering of a powder mix consisting of YSZ and LSM powders. It has been reported that the meso-scale microstructure of the porous composite cathodes is sensitive to the processing parameters such as the mean sizes of the initial powders [5,6] and sintering temperature [7,8], and the microstructure in turn affects the properties such as the polarization resistance and ohmic resistance that dictate the performance of the cathode. The key microstructural parameter that affects the electro-chemical response of porous LSM/YSZ cathodes is the total length of the LSM–YSZ–pores triple phase boundaries (strictly speaking, triple lines), i.e., TPB, in the three-dimensional (3D) microstructure per unit volume (i.e., the length density) because O_2 reduction and incorporation of O^{2-} into the electrolyte take place at these sites [9]. Accordingly, development of *quantitative* relationships among the processing parameters, microstructural geometry, and electro-chemical response of porous composite cathode materials is vital to the effective optimization of electrode performance. Clearly, to establish such quantitative correlations, it is imperative to observe all three microstructural constituents, namely, LSM, YSZ, and pores, *simultaneously* in the microstructure so that the microstructural features such as triple phase boundaries can be unambiguously identified and quantitatively characterized in an unbiased manner. Unfortunately, due to the microstructural length scales and the chemical nature of the phases in these microstructures, the conventional optical and scanning electron microscopy (SEM) techniques are not useful for simultaneous observations of all the three microstructural phases of interest in these materials. Optical microscopy is not useful due to sub-micron length scales of the grains, and the conventional SEM techniques are not useful because they do not provide sufficient contrast between YSZ and LSM phases due to their comparable average atomic numbers [10,11]. Although a high-resolution elec-

* Corresponding author. Tel.: +1 404 894 2887; fax: +1 404 894 9140.
E-mail address: arun.gokhale@mse.gatech.edu (A.M. Gokhale).

0378-7753/$ – see front matter © 2009 Elsevier B.V. All rights reserved.
doi:10.1016/j.jpowsour.2009.03.043

tron backscatter technique has been reported to yield sufficient contrast between YSZ and LSM phases in *coarse* microstructures produced via sintering at temperatures above 1200 °C [12], such coarse grained microstructures are not useful for SOFC applications. Recently, a combination of focused ion beam (FIB), Auger electron spectroscopy (AES) elemental mapping, and secondary electron imaging has been successfully used for imaging the YSZ and LSM phases [11]. Unfortunately, such equipments are not readily available in most research laboratories. Further, the use of FIB for the preparation of microstructural sections is very time consuming. Therefore, there is a need to further develop materialographic and microscopy techniques that enable unambiguous observations of all three microstructural constituents of interest, namely, electrolyte (such as YSZ), LSM, and pores, *simultaneously* in the microstructure using equipment that are readily available, *and* permit unbiased quantitative estimation of 3D microstructural parameters such as total length of triple phase boundaries per unit volume. In this contribution we report a combination of chemical etching technique and atomic force microscopy (AFM) that permits simultaneous observations of all three phases (i.e., YSZ, LSM, and porosity) as well as their triple phase boundaries in the microstructures of porous composite cathodes where YSZ and LSM phases have sub-micron size grains. In addition, a stereology based methodology [13–15] is presented for unbiased estimations of total length of the triple phase boundaries per unit volume and the total surface areas of interfaces of interest per unit volume in such 3D microstructures from simple counting measurements that can be performed on representative random two-dimensional (2D) microstructural sections. These stereological techniques are based on solid theoretical foundations rooted in stochastic geometry, and the basic equations involved have been known to mathematicians for more than a century [16–18]. The next section of the paper presents experimental details of material processing, materilography and atomic force microscopy (AFM) technique for microstructure observation, which is followed by description of the stereological techniques for estimation of total length of the triple phase boundaries and other microstructural parameters of interest.

2. Materials and methods

2.1. Materials and processing

The porous composite cathode material was fabricated via a powder processing route. The powders of YSZ (approximately 40% volume) and LSM (approximately 60% volume) were mixed and ground together using mortar and pestle for 30 min in ethanol to obtain a homogenous slurry that was subsequently dried at 75 °C. The mean powder sizes of the mixed and ground LSM and YSZ powders were 1.04 μm and 0.37 μm, respectively. The powder mix was hand-pressed to form pellets of 1 cm diameter and 1.5 mm height. These pellets were sintered at 1100 °C for 3 h to obtain a spatially uniform isotropic material containing the three phases, namely, YSZ, LSM, and porosity, and having the relative phase fractions and microstructural length scales in the same ranges as those in the porous composite cathodes of interest in the SOFC applications.

2.2. Materialography

The disc shaped porous composite cathode specimen was sectioned along a plane perpendicular to the faces of the disc for microstructural observations. The sectioned porous specimen was infiltrated with methylmethacrylate (MMA) in a vacuum chamber (Struers Epovac) at 150 mbar pressure for 2 min. The MMA infiltration was then polymerized under ultraviolet light at room temperature for 5 h. This leads to vacuum impregnation of the pores with MMA, which eliminates "pull-outs" of grains during subsequent polishing. The vacuum impregnated specimen was mounted in a cold-mounting epoxy for grinding and polishing. The mounted specimen was ground and polished using 240 and 800 grit SiC papers followed by fine polishing using diamond suspensions of different diamond sizes (9 μm, 6 μm, 3 μm and 1 μm). The final polishing was done using a colloidal silica suspension (0.05 μm size). The grinding and polishing steps were performed on Allied TechPrep polishing equipment. The polished sample was etched in a 3 M hydrochloric acid solution for 45 s at room temperature. As LSM and YSZ phases have different chemical reaction rates with hydrochloric acid, this etching procedure creates a small but consistent "relief" between the two phases, which can be detected by atomic force microscope and can be used to distinguish these phases in the microstructure.

2.3. Atomic force microscopy

Atomic force microscope (AFM) is a high-resolution scanning-probe equipment that scans nano-scale topography of the specimen surface using a miniature cantilever. The AFM records the extent of deflection of the cantilever as the tip traverses the specimen surface, and thereby, generates a topographic map of the surface. The *Z* (depth) resolution of AFM is typically 1 nm, and therefore, a differential topographic "relief" between microstructural phases (YSZ and LSM in the present case) on the order of nanometers generated by chemical etching can be precisely detected by AFM. The resulting topographic map can be used to visualize the chemically etched microstructure of porous composite cathode containing YSZ, LSM, and porosity phases. In the present study, a Veeco Dimensions 3100 AFM equipped with VL 300-A Phosphorous (n) doped Si cantilever having front angle of 15° and tip height of 15 μm was used. The images were recorded in tapping mode with a sampling frequency of 1 Hz, *X*–*Y* resolution of 20 nm, and Z resolution of 1 nm. At this resolution, each AFM image (topographic map) of a microstructural area of 100 μm^2 containing about 400 YSZ and LSM grains and about 500 triple phase boundaries could be recorded in about 8 min. The grain sizes of YSZ and LSM grains are on the order of 400 nm, and therefore, the *X*–*Y* resolution of 20 nm and *Z* resolution of 1 nm are quite sufficient to clearly observe the microstructure.

2.4. Digital image processing

Digital image processing transforms a raw AFM data set (topographic map) into the corresponding microstructural image. To generate gray-scale microstructural images, the Gwyddion image processing software package was used. This image processing step transforms topographic AFM data into a gray-scale image of the microstructure, where the gray-scale assigned to a pixel is directly related to the topographic height at that point. The resulting image consists of 256 gray scales. In the present case, a nonlinear rendering was employed to enhance the contrast. For automated quantitative microscopic measurements it is essential to "segment" the gray-scale image and create a three-color map of the microstructure; one color for each of the phases YSZ, LSM, and porosity. This segmentation was performed by using an in-house computer code implemented in the KS-400 image analysis system. Very small features (smaller than 0.012 μm^2 area) were removed (scrapped) from the segmented images to eliminate the noise in the microstructural images, and then the quantitative microstructural measurements were performed.

2.5. 3D microstructure characterization

Once a segmented image of 2D microstructural section is generated, numerous quantitative measurements can be performed

on the microstructural features automatically using commercial image analysis software packages. Nonetheless, it is the 3D microstructure and its geometric properties that are of fundamental interest. Stereological techniques [13–15] that involve applications of well-known stochastic geometry and statistical sampling theories [16–18] enable statistical *estimations* of numerous attributes of any 3D microstructure from certain specific measurements that can be performed on representative random 2D sections through the 3D microstructural space of interest. These techniques are unbiased, general, and assumption-free, and therefore, they can be applied to any microstructure encountered in materials science [13] as well as in biology [19]. In the context of SOFC porous composite cathode microstructures, the following 3D microstructural parameters are of interest:

1. Total length of triple phase boundaries (lines common to YSZ, LSM, and pores) in the 3D microstructure per unit volume.
2. Total surface areas of YSZ-pore, LSM-pore and YSZ-LSM interfaces per unit volume.
3. Volume fractions of YSZ, LSM, and pore phases in the microstructure.

Interestingly, all the above 3D microstructural attributes can be estimated from the measurements performed on representative random 2D microstructural sections using the following equations, which have been known for more than 50 years [13–15]. Note that these estimations involve simple "counting" measurements that can be also performed automatically using image processing and the sampling errors in all the estimates can be computed using standard techniques [13–15]:

$$T_V = 2\langle Q_A \rangle \quad (1)$$

In Eq. (1), T_V is the total length of the triple phase boundaries in 3D microstructure per unit volume and $\langle Q_A \rangle$ is the average value of the number of triple junctions (i.e., junctions of YSZ, LSM, and pore phases) in 2D sections per unit area, which can be measured experimentally. The total surface area per unit volume for any type of interfaces (for example, YSZ–LSM interfaces) of interest S_V can be estimated by using the following well-known stereological relationship:

$$S_V = 2\langle I_L \rangle \quad (2)$$

In Eq. (2), $\langle I_L \rangle$ is the average value of the number of intersections between the interfaces of interest and random test lines per unit test line length. The volume fraction of a phase (for example, LSM) V_V can be estimated by using the following equation:

$$V_V = \langle A_A \rangle \quad (3)$$

$\langle A_A \rangle$ is the average value of the area fraction of the phase of interest in 2D sections. The volume fraction of a phase is therefore estimated by measuring the area fraction of the phase in 2D sections. The area fraction of each phase is measured by dividing the total number of pixels of each phase by the number of pixels in the digital image (512×512 in the present case). In the present study, the triple phase boundary length per unit volume, the volume fractions of all the three phases (YSZ, LSM, and pores), and the total surface area interfaces between YSZ and pores, LSM and pores, and YSZ and LSM in the 3D microstructure per unit volume were estimated by performing the required measurements on a statistical microstructural sample consisting of seven representative random segmented AFM images each covering microstructural area of $10\,\mu m \times 10\,\mu m$ recorded with a X–Y resolution of 20 nm. These images contained approximately 2700 YSZ and LSM grains and 3500 triple phase boundary junctions, and therefore, constitute a large statistical sample. Consequently, the statistical estimates of the microstructural parameters obtained from these images are expected to be robust and reliable. These data are reported and discussed in the next section.

3. Results and discussion

Fig. 1(a) depicts a gray-scale AFM image showing the three phases YSZ, LSM, and pores. In this image, the bright phase is YSZ, the darkest phase is the porosity, and the gray phase is LSM. Thus, atomic force microscopy enables clear distinction among the three phases. Fig. 1(b) shows segmented color-coded image of the microstructural field in Fig. 1(a); the quantitative stereological measurements were performed on such segmented images in an automated manner using image processing. The estimated values of volume fractions of the three phases, total surface area per unit volume of the YSZ–pore, LSM–pore, and YSZ–LSM interfaces per unit volume, and the corresponding statistical sampling errors are given in Tables 1 and 2. The total length of the triple phase boundaries per unit volume (i.e., the length density) estimated from the measurement performed on the color-coded AFM images and application of Eq. (1) is $10.8 \pm 1.15\,\mu m\,\mu m^{-3}$. The estimated porosity of the composite cathode is 46%. Note that the present pro-

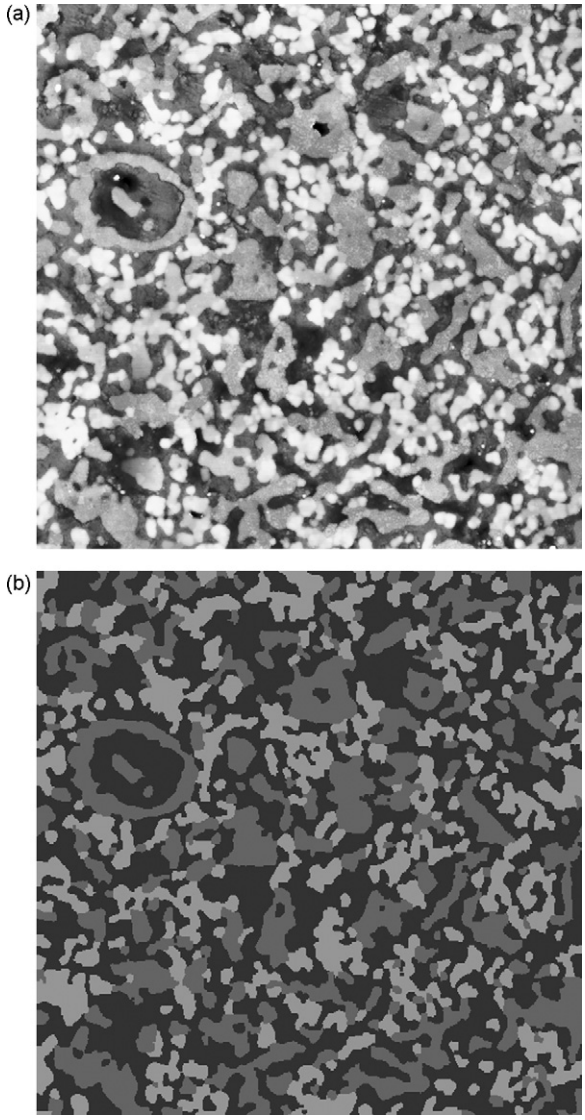

Fig. 1. AFM image of the etched surface: (a) rendered AFM image; (b) color-coded segmented image. In both images the bright phase is YSZ, the gray phase is LSM, and the darkest phase is porosity.

Table 1
Measurements of volume fraction of each phase. Porosity is calculated as the remaining volume fraction aside from YSZ and LSM.

	YSZ	LSM	Porosity
Volume fraction	0.28	0.26	0.46
Sampling error	0.027	0.018	

cedure for the estimation of triple phase boundary length per unit volume does not require reconstruction of opaque 3D microstructure. Wilson et al. [20] carried out detailed 3D microstructure reconstructions of numerous composite porous cathodes of different compositions containing YSZ, LSM, and pore phases using FIB based serial sectioning and backscattered SEM based imaging of the serial sections. They estimated the triple phase boundary length per unit volume to be in the range of 8–10 $\mu m\,\mu m^{-3}$. Therefore, the present data are in the same range as those reported by Wilson et al. on reconstructed 3D microstructures. Nonetheless, the present technique does not require advanced SEM-based imaging procedures; serial sectioning using FIB (which is an extremely slow process); and reconstruction of 3D microstructure. Therefore, the present AFM based microstructure observations and stereology based estimations of the microstructural properties are very efficient for simultaneous observations and quantitative characteri-

Table 2
Measurements of interface/surface areas per unit volume ($\mu m^2\,\mu m^{-3}$).

	YSZ/pore (S_1)	LSM/pore (S_2)	YSZ/LSM (S_3)	Total surface area (S_1+S_2)
Interface area ($\mu m^2\,\mu m^{-3}$)	3.9	2.3	0.63	6.2
Sampling error	0.21	0.30	0.09	

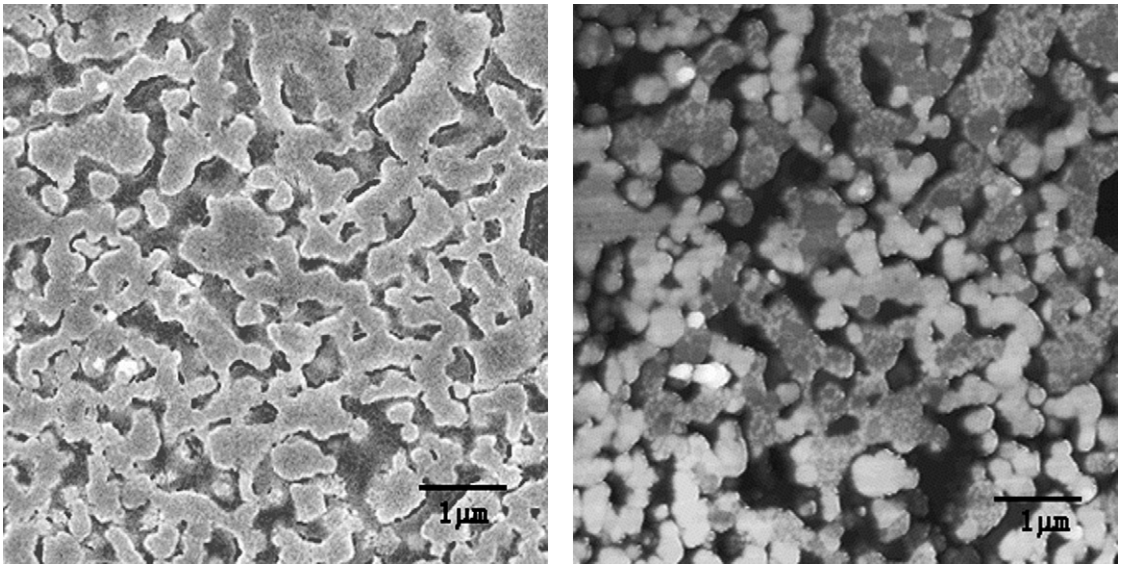

Fig. 2. SEM (left) and AFM (right) images of the marked area.

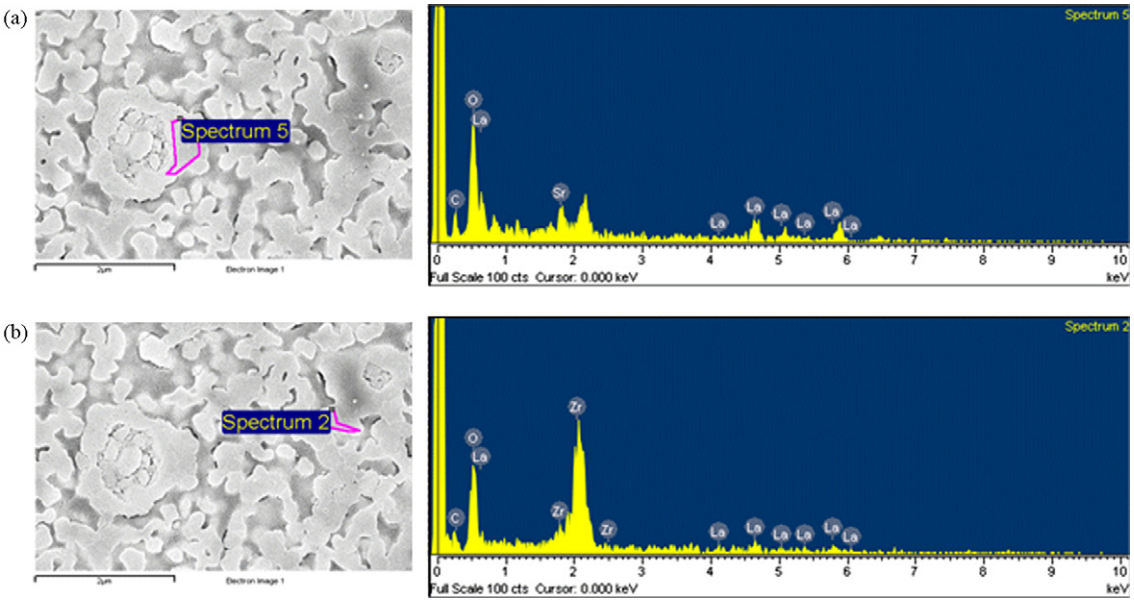

Fig. 3. EDS analysis of the selected regions: (a) LSM region and (b) YSZ region.

zation of the three phases (YSZ, LSM, and pores) and the triple phase boundaries in the composite porous cathode microstructures. The present technique is also applicable for region specific quantitative characterization of SOFC composite cathode microstructure. When the microstructure near the interface between the solid electrolyte (YSZ) and porous composite cathode membrane is of interest, it can be separately characterized by performing the measurements only in that region. It is of interest to validate the present AFM based microstructural observation technique. For this purpose, four microhardness indents were placed in one region of a polished and etched specimen as markers and gray-scale AFM and SEM (Joel 1530, InLens mode) images of exactly the same region were recorded, which are depicted in Fig. 2. Observe that the porosity distribution in both the micrographs appears to be identical; the only difference between the two micrographs is that the YSZ and LSM phases cannot be distinguished in the SEM image. To further confirm the AFM based microstructural observations, energy dispersive spectra (EDS) were used to identify the phases in the polished sample surfaces based on their elemental compositions (see Fig. 3). For YSZ/LSM composite, yttrium and lanthanum were selected as the indicative elements of YSZ and LSM, respectively. Regions of interest were chosen based on their local topographic height differentials with respect to the neighboring phases created by chemical etching. In Fig. 3(a) the EDS signal was collected from a low topographic region with respect to its surrounding features. Such topography indicates that this region is LSM. The EDS spectrum shows lack of zirconium and a more pronounced lanthanum peak and confirms the presence of LSM phase at that spot. In Fig. 3(b), the EDS signal was collected from a raised region near a step. Such topography indicates that this region is YSZ. The strong zirconium peak in the EDS spectrum confirms the presence of the YSZ phase at that location. Therefore, these EDS observations validate the topography based distinctions between YSZ and LSM phases generated by AFM for simultaneous observations of YSZ and LSM phases (and porosity) in the composite porous cathode microstructures.

4. Summary and conclusions

A simple and practical technique has been developed for simultaneous observations of all three phases (YSZ, LSM, and porosity) in the microstructure of porous composite cathode materials for SOFC applications. It is shown that this AFM-based microstructure imaging technique also provides a viable and efficient methodology for quantitative characterization of the 3D microstructures of YSZ/LSM composite cathode materials when combined with unbiased stereological measurements. Microstrucutral parameters such as total triple phase boundary length per unit volume, volume fractions, and surface areas can be estimated from the measurements performed on AFM based images of the 2D microstructural sections without tedious and time consuming reconstruction of 3D microstructures.

Acknowledgements

This research was supported through a grant from the U.S. National Science Foundation (NSF grant DMR-0813630) for which Dr. B. MacDonald and Dr. A.J. Ardell are the Program Managers. The financial support is gratefully acknowledged. The views and conclusions contained herein are those of the authors and should not be interpreted as necessarily representing the official policies or endorsements, either expressed or implied, of the funding agency or the US government.

References

[1] M. Juhl, S. Primdahl, C. Manon, M. Mogensen, J. Power Sources 61 (1996) 173–181.
[2] M.J. Jorgensen, M. Mogensen, J. Electrochem. Soc. 148 (2001) A433–A442.
[3] V. Dusastre, J.A. Kilner, Solid State Ionics 126 (1999) 163–174.
[4] E.P. Murray, S.A. Barnett, Solid State Ionics 143 (2001) 265–273.
[5] H.S. Song, W.H. Kim, S.H. Hyun, J. Moon, J. Electroceram. 17 (2006) 759–764.
[6] H.S. Song, W.H. Kim, S.H. Hyun, J. Moon, J. Kim, H.W. Lee, J. Power Sources 167 (2007) 258–264.
[7] K. Sasaki, J.P. Wurth, R. Gschwend, M. Godickemeier, L.J. Gauckler, J. Electrochem. Soc. 143 (1996) 530–543.
[8] M.J. Jorgensen, S. Primdahl, C. Bagger, M. Mogensen, Solid State Ionics 139 (2001) 1–11.
[9] J. Fleig, Annu. Rev. Mater. Res. 33 (2003) 361–382.
[10] C.Y. Wang, Y.L. Liu, R. Barfod, S.B. Schougaard, P. Gordes, S. Ramousse, P.V. Hendriksen, M. Mogensen, Risø International Symposium on Materials Science: Solid State Electrochemistry, Denmark, 2005.
[11] L.A.L. Tarte, J.R. Cournoyer, K. Dovidenko, E.J. Olson, J.A. Ruud, T. Striker, Microsc. Microanal. 11 (2005).
[12] C.C.T. Yang, W.C.J. Wei, A. Roosen, Mater. Chem. Phys. 81 (2003) 134–142.
[13] A.M. Gokhale, ASM Handbook: Metallography, and Microstructures, vol. 9, 2004, pp. 428–447.
[14] R.T. DeHoff, F.N. Rhines, Quantitative Microscopy, McGraw Hill Publishing Co., New York, NY, 1968.
[15] E.E. Underwood, Quantitative Stereology, Addison Wesley Publishing Co., Reading, MA, 1970.
[16] J. Ohser, F. Muecklich, Statistical Analysis of Microstructures in Material Science, John Wiley & Sons, New York, 2000.
[17] L.A. Santalo, Integral Geometry and Geometric Probability, Addison-Wesley Publishing Co., Reading, MA, 1976.
[18] D. Stoyan, S. Kendall, J. Mecke, Stochastic Geometry and its Applications, 2nd ed., John Wiley and Sons, NY, 1995.
[19] P.R. Mouton, Principles and Practices of Unbiased Stereology: An Introduction for Bioscientists, The Johns Hopkins University Press, Baltimore, MD, 2002.
[20] J. Wilson, A. Duong, J. Cronin, M. Gameiro, S. Rukes, K.H. Chen, D. Mumm, S. Barnett, 33rd International Conference & Exposition on Advanced Ceramics & Composites, 2009.